ACADEMIA JOURNAL OF BIOLOGY 2026, 48(1): 53–65
DOI: 10.15625/2615-9023/21739

IRON (II) AND ZINC (II) CHELATING ABILITIES OF PEPTIDES FROM SPENT BREWER'S YEAST

Thi Bich Ngoc Ha, Thuy Hang Dam, Thi Lan Phuong Tran, Thi Hong Hanh Tran, Kim Anh To, Tuan Anh Pham, Tuan Le*

Department of Bioengineering, School of Chemistry and Life Sciences, Hanoi University of Science and Technology, Vietnam

Received 17 October 2024; accepted 6 March 2026

ABSTRACT

Zinc and iron are essential microelements that contribute to a wide range of physiological functions in humans and animals. However, their inorganic forms often have low solubility and bioavailability and leading to zinc and iron deficiency. The alternative chelated forms of these essential metals offer a high absorption rate and bioavailability of these two metals in humans and animals. Spent brewer's yeast is considered a low-cost by-product of the brewing industry that contains high concentrations of proteins and can be used to generate zinc and iron-peptide chelate as value-added products. The purpose of this study was to investigate the potential of chelating zinc and iron using peptides resulting from spent brewer's yeast. Our results showed that protein concentration and degree of hydrolysis increased the zinc and iron chelating ability. The peptide fraction of less than 3 kDa demonstrated a maximum chelating yield exceeding 80% at pH 7. FTIR analysis revealed that the possible chelating site might be at the C=O of the carboxyl group and the C-N or N-H of amide-I and amide-II groups.

Keywords: Metal chelating peptide, spent brewer's yeast, zinc, iron.

Citation: Thi Bich Ngoc Ha, Thuy Hang Dam, Thi Lan Phuong Tran, Thi Hong Hanh Tran, Kim Anh To, Tuan Anh Pham, Tuan Le, 2026. Iron (II) and zinc (II) chelating abilities of peptides from spent brewer's yeast. *Academia Journal of Biology*, 48(1): 53–65. https://doi.org/10.15625/2615-9023/21739

**Corresponding author email*: tuan.le1@hust.edu.vn

INTRODUCTION

Zinc and iron are essential components of more than 300 different enzymes and owe their catalytic effect to their direct involvement in substrate conversion and the stabilization of enzyme structures. They exert structural effects on several transcription factors and regulate hormoves, hormone receptors and gene expression. Therefore, they play important roles in many biochemical and physiological processes in cells and are proven to have an influence on metabolism, growth and development of animals. Deficiency in zinc and iron is one of the most common nutritional disorders in humans and animals, which can lead to mild to severe consequences such as chronic anemia, neural degeneration, chronic kidney disease and susceptible to infection (Maret, 2004; Abbaspour et al., 2014). Mineral deficiency often results from insufficient intake, impaired absorption or the low solubility, bioaccessibility and bioavailability of minerals in the human and animal's intestine, especially when inorganic minerals are used as supplements and for food fortification in human and animal diets (Oliveira et al., 2023).

As an alternative for inorganic mineral supplements, metal chelating peptide (MCP) has several advantages which have been verified *in vivo*: (i) MCP can avoid to be precipitated during the gastrointestinal digestion by keeping away adverse effects of other nutrients especially phytic acid and fiber; (ii) MCP can be absorbed via the intestinal epithelial cells through peptide transporter (PepT1) channel and/or vesicle mediated transcytosis which are more stable, faster, and have lower energy consuming. In comparison, other forms of metals are mainly absorbed by the intestinal mucosal cells through an "ion pathway" in the intestine (Udechukwu et al., 2018) (iii) MCP derived from food resources has low cost and has no side effects such as nausea, abdominal pain, and loss of appetite which are often observed on metal salts (Zhang et al., 2018). Protein hydrolysates, which are rich in structural features such as carboxyl groups, sulfhydryl groups, negative charges, and ionic bonds in peptides could improve the metal chelating ability. Peptides containing His residues play an important role in metal chelation (Sun et al., 2020). In addition, Cys, Glu, Ser and Asp residues containing S, O and N atoms are also involved in the formation of MCP (Caetano-Silva et al., 2015). In addition to the amino and carboxyl head groups, the main amino acid side chain groups that bind metals are the carboxyl group of Asp and Glu, the imidazole group of His, the hydroxyl group of Ser, the sulfhydryl group of Cys, the ε-amino group of Lys and the guanidine group of Arg (Wang et al., 2014; Lv et al., 2017). In addition, protein hydrolysates are now also considered a source of biologically active peptides. They exhibit antibacterial, antioxidant, hypocholesterolemic, immunomodulatory, as well as hypotensive and mineral absorption enhancing activities (Mirzaei et al., 2015).

Because of the interaction between amino acids and metal ions, the choice of protein sources for metal chelation depends on the availability of amino acids in the peptide that can form an interaction with the metal ions added. In general, ferrous ions can form chelation with carboxylic groups, especially from Glu and Asp, which can be found in a variety of protein sources. Chelation of peptides with ferrous ions has been studied using a wide range of protein sources, including mungbean, oat, corn gluten, whey protein, soybean (Athira et al., 2021; Yuanqing et al., 2021; Zhang et al., 2021; Qu et al., 2022). Proteins from oysters, fish, pine nut, and coconut cake have been used to form zinc-peptide chelates (Guo et al., 2021; Peng et al., 2023; Zhang et al., 2023; Zheng et al., 2023). Another consideration when choosing protein sources is the availability in bulk and cost. In that sense, byproducts from the food industry have been proven to be a great choice.

Spent brewer's yeast (SBY), also known as residual yeast or surplus yeast, is a prevalent by-product of the brewing industry, created when the yeast used in fermentations is no longer useful and must be disposed of. It is estimated that 15 to 18 tons of surplus yeast are produced per 10,000 hL of finished beer.

Other major by-products include brewer's spent grains and hot trub. SBY is a rich source of B vitamins, proteins (45–60%) and other compounds that could be applicable to both food and non-food products. However, the high level of nucleic acids in SBY limits its use as a protein supplement in humans due to the negative health effects caused by an excess of uric acid (Podpora et al., 2016). Therefore, SBY is mainly utilized in animal feed formulations as a low-cost source of protein. SBY is a high-protein by-product. It contains 45–60% protein and is generally regarded as safe (GRAS). SBY was found to contain more than 60 % protein (dry weight) with a high percentage of essential amino acids (Podpora et al., 2016; Vieira et al., 2016). Currently, the most well-known and commonly used outlet for SBY is as a constituent of animal feeds, mainly as a cheap source of protein, as well as a source of minerals and B vitamins. SBY may be incorporated as a wet slurry or can be dried before feeding. The addition of yeast to animal feeds has been shown to have positive effects on feed quality and feed utilization (Jaeger et al., 2020).

In essence, SBY is an underutilized brewing by-product with a variety of exciting potential applications in the food industry and beyond. Increased awareness of this potential may instigate further research into these new applications and create new opportunities for their exploitation. This study aims to investigate the zinc and iron chelating abilities of peptides from SBY and the conditions of chelating reactions.

MATERIALS AND METHODS

Spent brewer's yeast

Spent brewer's yeast (*Saccharomyces pastorianus*) was collected from Habeco Co. Ltd. After being transferred to the laboratory, SBY was washed twice by mixing distilled water (ratio 1 : 2 by volume) at 4 ^{o}C, followed by centrifugation at 6000 RPM to remove the supernatant. The washed spent brew yeast was stored at -20 ^{o}C for further experiments. The SBY represents 57.83 ± 2.00% of total protein (determined by the Kjeldahl method with conversion factor k = 6.25) and water content of 79.02 ± 0.321%.

Bead mill

SBY (humid matter) was mixed with distilled water at a ratio of 1:1 by weight (equivalent to 10.5% dry weight). Then 0.9 g of SBY slurry was mixed with 0.45 g of Ø 0.5 mm glass bead, 0.45 g of Ø 1 mm bead, and 2 beads of Ø 3.5 mm in the milling tube. Each cycle corresponds to 20 sec milling (Mini-Beadbeater, Biospec) and 60 sec cooling down in ice. Milled SBY samples were centrifuged at 10.000 RPM, 10 min, and supernatants were collected and stored at 4 ^{o}C for further experiments.

Autolysis and enzymatic hydrolysis

The autolysis of SBY was performed at 7% solid loading (dry matter), at pH 6.0, temperature 50 ^{o}C, mixing rate of 600 RPM in a Biostat B plus bioreactor for 12 hours. The working volume was 1,000 mL. Samples were periodically taken and immediately treated in boiling water for 10 min to inactivate enzymes, then centrifuged at 10,000 RPM for 10 min. Supernatant obtained from autolysis was transferred to a Biostat B plus bioreactor for hydrolysis using Alcalase (Novozymes, dosage 30 mg/g protein). The hydrolysis was performed at pH 8.0, 55 ^{o}C, 600 rpm for 8 hours.

Cross flow filtration (CFF)

SBY hydrolysate was first centrifuged at 10.000 RPM for 15 min, then the precipitate was removed. Supernatant was sequentially fractionated by micro and ultra-filtration (Quixstand bench-top CFF systems) using different filter cartridges of 0.2 µm (CFP-2-E-3MA), 100 kDa (UFP-100-E-3MA), 10 kDa (UFP-10-E-3MA), and 3kDa (UFP-3-C-3MA). After each step, the permeate (Pe) was collected for further experiments.

Chelating reaction and evaluation of the chelating ability

Chelating reactions were performed in micro-scale by mixing 50 µL of metal ion stock

solutions ($FeCl_2$ from 300 mM to 1,500 mM or ZnCl2 from 150 mM to 800 mM) with 950 µL of SBY peptide solution for 60 seconds using a vortex mixer, then centrifuged at 10.000 rpm for 5 min to remove precipitation (if it existed). For the negative control, the metal stock solution was replaced by distilled water. For the positive control, the SBY peptide solution was replaced by distilled water. The concentration of free Zn^{2+} was determined based on the reaction with 4-(2-pyridylazo) resorcinol, and absorbance was read at 500 nm (Zhang & Ye, 2022) using a GeneQuant 1,300 spectrophotometer. The concentration of free Fe^{2+} was determined based on the reaction with 10-Orthophenanthroline, and absorbance was read at 510 nm (Xu et al., 2022). The amount of chelated ion (µg/mL or µg/mg protein) was calculated as the difference between the total metal ion loaded and the free ion measured after the reaction was done. The chelating yield (%) is defined as the ratio between the chelated ion on the total ion loaded.

Yeast cell analysis

SBY samples taken during bead mill and autolysis were diluted with distilled water, then observed on a microscope at 40 magnification (Nikon Eclipse E100). The number of undamaged cells was counted from 10 observations for each sample.

Analysis of the SBY peptide

Soluble protein was measured using the Lowry method. The concentration in alpha-amino was determined by using the ninhydrin reaction in the presence of pyridine (Friedman, 2004). The reaction composition included 50 µL of sample, 500 µL of 2% ninhydrin, and 500 µL of 20% pyridine.

Fourier-transform infra-red (FTIR) and UV-Vis spectroscopy analysis

Samples for FTIR analysis were prepared using the ethanol precipitation method (Xu et al., 2022; Fan et al., 2023; Liu et al., 2024). One volume of either iron-chelating peptide (FeCP) or zinc-chelating peptide (ZnCP) solutions were mixed with four volumes of absolute ethanol. After 4 hours incubated at 4 ^{o}C, the mixture was centrifuged at 10,000 RPM for 15 min. Precipitate was then washed 4 times using absolute ethanol, then vacuum dried at 45 ^{o}C to obtain FeCP and ZnCP in powder form. FTIR spectrum of the samples was analyzed by the NICOLET IS20 (Thermo Fisher Scientific, USA) and measured in attenuated total reflectance (ATR) mode, ranging from 500 to 4,000 cm^{-1}. UV-Vis spectra of peptide and metal chelating peptide solutions were performed using a Jasco V-750 spectrophotometer. Particle size distribution of samples was carried out by Nanosizer Pro (Malvern) with a material refractive index of 1.45 (protein) and dispersant refractive index of 1.33 (water).

Particle size distribution

The particle size distribution analysis was performed on Nanosizer Pro (MAL1257886, Malvern) with the material refractive index of 1.45 (refer to protein) and the dispersant refractive index of 1.33 (refer to water). The temperature and sample equilibre time were 25 ^{o}C and 30 seconds, respectively.

Data analysis

All experiments were repeated at least three times. The data were first evaluated by descriptive statistics using the Megastat add-in (Microsoft Office Excel), and outliers were excluded. Secondly, the Duncan test was applied to evaluate the significant difference of means with $p < 0.05$ (SPSS software).

RESULTS AND DISCUSSION

Extraction of proteins and peptides from SBY

It was observed that the bead mill method effectively breaks SBY cells, resulting in a significant increase in soluble protein concentrations after the 1st and the 2nd cycle (Fig. 1). This evolution was in good agreement with microscopic analysis that indicated less than 49% of SBY cells were undamaged after 2 milling cycles. After 4 milling cycles, 93.23 ± 2.89% of SBY cells were damaged. This observation was similar

to the reported result of Jacob et al. (2019). The decrease in soluble protein concentration after 3 and 4 cycles can be explained by the denaturation of proteins due to mechanical force, as reported by Liu et al. (2016).

Using the biological method, the autolysis of SBY yielded 34.56 ± 4.65 g/L of soluble protein after 8 h, corresponding to a ratio of 14.8% normal cells. From this point, further extension of the autolysis duration up to 24 hours did not result in any significant improvement in soluble protein concentration (Fig. 2). In a similar study, Jacob et al. (2019) reached a higher cell disruption yield of 98% after 24 hours of autolysis.

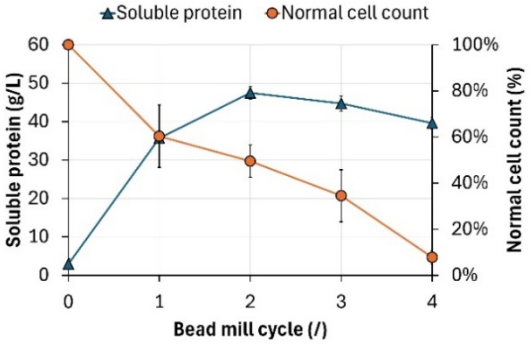

Figure 1. Extraction of protein from SBY at 10.5% solid loading using the bead mill method

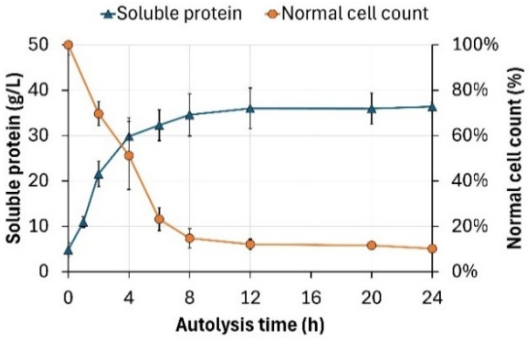

Figure 2. Extraction of protein from SBY at 7% solid loading using the autolysis method

With the bead mill method, soluble protein reached 47.46 ± 1.64 g/L after 2 milling cycles, which was higher than the obtained value by autolysis (34.56 ± 4.65 g/L after 8 h). However, as bead milling was carried out at higher solid loading, the protein extraction yield was only 0.405 ± 0.014 g protein/g dm SBY. This number is approximately 20% lower than that by the autolysis method, which reached 0.494 ± 0.066 g protein/g dm SBY. Compared to autolysis, the bead milling method also requires higher energy input and complex equipment at large-scale processes. Thus, autolysis appeared as the most suitable method for extracting protein from SBY.

Chelating ability of SBY peptides

Figure 3 & 4 represent the chelating ability of SBY peptide solutions obtained during autolysis and hydrolysis with iron (II) and zinc (II), respectively. During the first 4 hours of autolysis, the chelating ability of SBY peptide increased for both iron and zinc, which may be due to a significant increase in soluble protein concentration (Fig. 2). It is interesting that during enzymatic hydrolysis, the increasing trend in both iron and zinc chelating ability was recognized. Together with the analysis of α-amino, it is suggested that the hydrolysis of peptide bonds by protease creates new α-amino and α-carboxyl groups, which can be the possible binding site for metal ions. A similar conclusion was also drawn from other studies (Wang et al., 2011; Wang et al., 2020). However, over-hydrolysis may result in a decrease in chelating ability due to the conversion of small peptides to single amino acids. Thus, both protein concentration and the degree of hydrolysis were important to facilitate the highest chelating ability of iron (II) and zinc (II).

The soluble protein concentration in the hydrolysate (H8) was 35.09 ± 0.15 g/L. After the 0.2 µm microfiltration and 100 kDa cut-off, this value slightly decreased to 34.78 ± 2.03, indicating the small proportion of high molecular weight protein in the hydrolysate of SBY. Through the 10 kDa and 3 kDa cut-off, the concentration of soluble protein was reduced significantly to 28.74 ± 0.72 g/L and 24.45 ± 1.88 g/L, respectively. The chelating

ability of the SBY peptide was boosted through each cut-off filtration step (Fig. 5), and the highest value was obtained from the fraction with MW ≤ 3 kDa. Previous studies also reported the best chelating ability of peptides smaller than 3 kDa derived from mung bean (Fu et al., 2020) and peanut proteins (Li et al., 2020). It is possible that for higher MW peptides or for protein molecules with bulky 3D structure, only chemical groups on their surface can freely interact with metal ions, while certain limitations may exist for the inner counterparts. Our achievement was better than 14.32 mg Fe/g protein obtained by Zang & Ye (2022) and 30.8 mg Zn/g peptide obtained by Zheng et al. (2023).

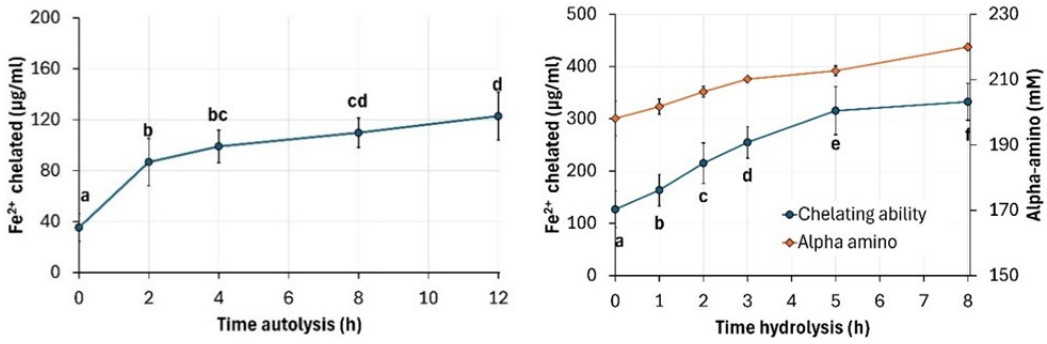

Figure 3. Iron (II) chelating ability of SBY peptides during autolysis and hydrolysis. Total Fe^{2+} loaded was 1,120 µg/mL

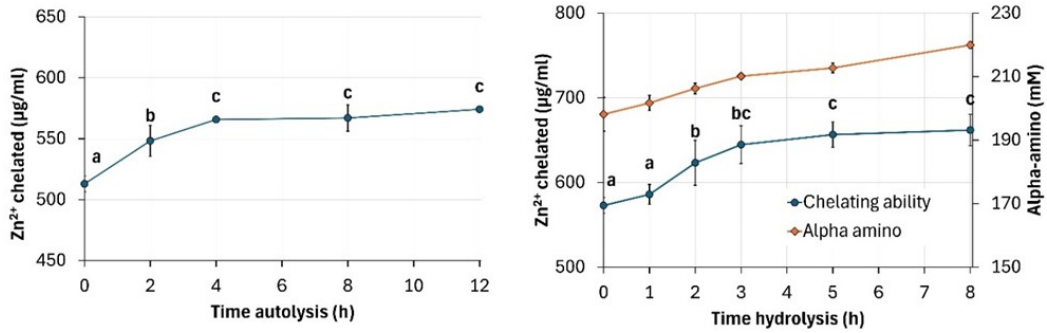

Figure 4. Zinc (II) chelating ability of SBY peptides during autolysis and hydrolysis. Total Zn^{2+} loaded was 812.5 µg/mL

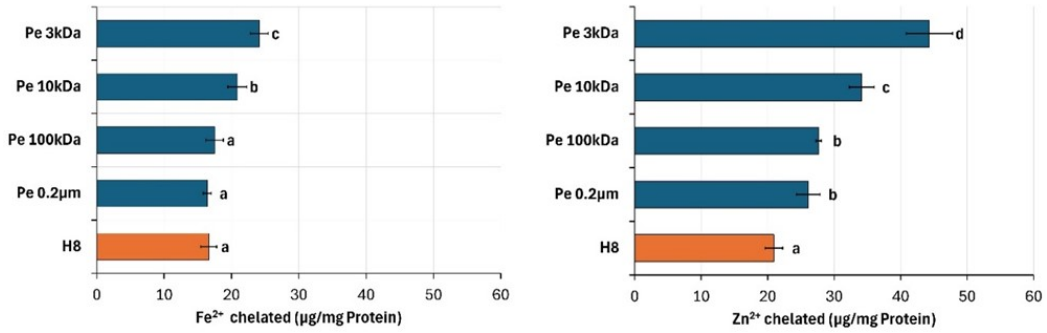

Figure 5. Chelating ability of SBY hydrolysate (H8) and its CFF permeate fractions (Pe 0.2 µm, Pe 100 kDa, Pe 10 kDa, Pe 3kDa). Fe^{2+} loading was 2,240 µg/mL, Zn^{2+} loading was 1,625 µg/mL

Chelating conditions

The evaluation of chelating conditions was performed using the 3 kDa permeate fraction. Among several criteria, pH is a crucial factor for the formation of metal-peptide complexes (Zhang et al., 2018). From pH 4.0 to 7.0, the iron chelating ability showed a gradual increase and reached the highest peak at pH = 7.0 (Fig. 6). At alkaline pH, the amount of chelated iron (II) cannot be accurately measured due to the formation of $Fe(OH)_3$ precipitation. The zinc chelation rate increased as the pH approached the neutral point, and the highest value was achieved at pH 7. At low pH, the abundance of H^+ in the reaction medium may compete with metal ions to interact with the electron receptors. In contrast, high pH values may enhance the coordination between metal cations and negatively charged carboxyl groups of peptides. However, it also generates competition between carboxyl groups of peptide molecules and free hydroxyl groups in the solution to create chemical bonds to metal cations (Fang et al., 2020). Thus, neutral pH seems to be the best condition, and several authors have chosen this condition for chelating reaction (Shi et al., 2021; Zhang et al., 2021; Jiang et al., 2022). However, a slightly different conclusion can be found in the literature regarding oat peptide, which showed the best iron chelating ability at pH = 6 (Yuanqing et al., 2021).

It was reported that the chelating yield increased proportionally to the metal ion loading until reaching a certain steady state, then an over-dose of metal ion may lead to a decline in peptide chelate formation (Athira et al., 2021; Yuanqing et al., 2021). Our results (Fig. 7) indicated that the amount of chelated iron (II) or zinc (II) increased at a higher metal loading ratio, but the chelating yield tends to decrease.

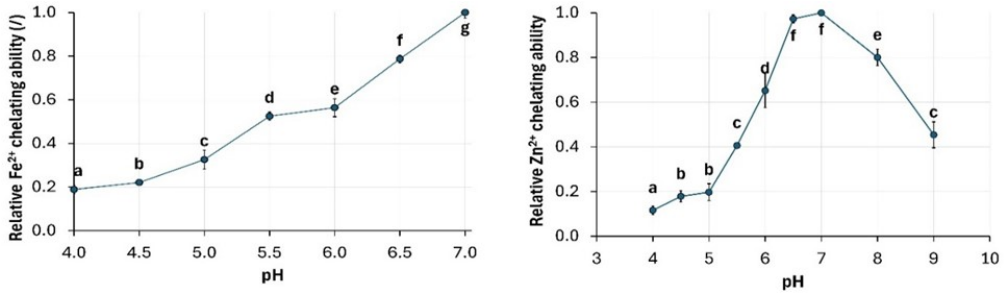

Figure 6. Effect of pH on the chelating ability of SBY peptide to Fe^{2+} and Zn^{2+}. Maximum chelating ability was taken as 1. Fe^{2+} loading was 2,240 µg/mL, Zn^{2+} loading was 812.5 µg/mL

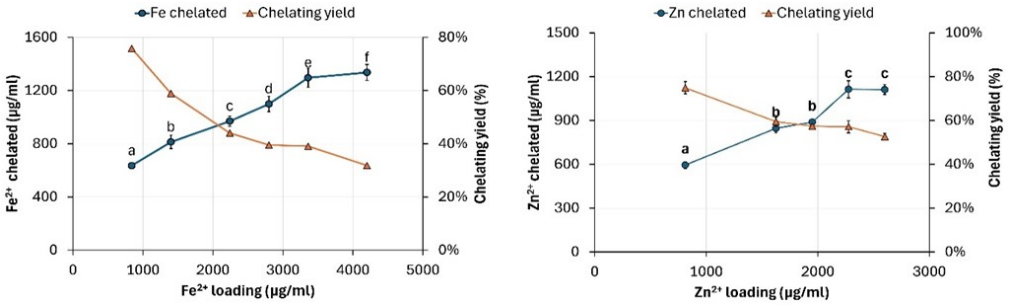

Figure 7. Effect of initial metal ion loading on the chelating ability of SBY peptide to Fe^{2+} and Zn^{2+}

A suitable heat treatment is advantageous for producing the metal-peptide complex by supplying energy for the reaction since the interaction between peptide and metal ions is an endothermic process. High temperature (50 ^oC)

significantly speeds up the formation of FeCP (Fig. 8), but it might cause parts of the complex to be destroyed in the case of ZnCP (Fig. 8). It was also concluded that the zinc chelating reaction occurred at a very high rate, reaching its maximum yield within 10 min. For the interaction between iron and SBY peptide, the process required 40 to 60 min, depending on reaction temperature, to reach the saturation concentration.

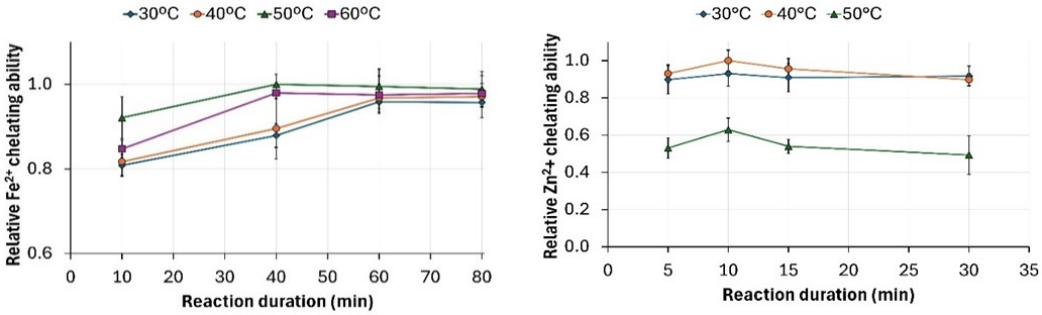

Figure 8. Effect of reaction time and temperature on the chelating ability of SBY peptide to Fe^{2+} and Zn^{2+}. Maximum chelating ability was taken as 1. Fe^{2+} loading was 2,240 µg/mL, Zn^{2+} loading was 812.5 µg/mL

UV-Vis and FTIR spectrum of FeCP and ZnCP

The changes in the peak of SBY peptide have been observed, being from 206.5 nm before binding to metal ions to 206.0 nm and 205 nm after binding to ferrous ion and zinc ion, respectively. The second peak of the peptide at 258.5 nm did not change after binding to ferrous ion, but was shifted to 259 nm after the chelating reaction with zinc ion (Fig. 9). Our observation was similar to those in previous studies, confirming that both ferrous ion and zinc ion were successfully chelated to SBY peptides (Peng et al., 2023; Fan et al., 2022).

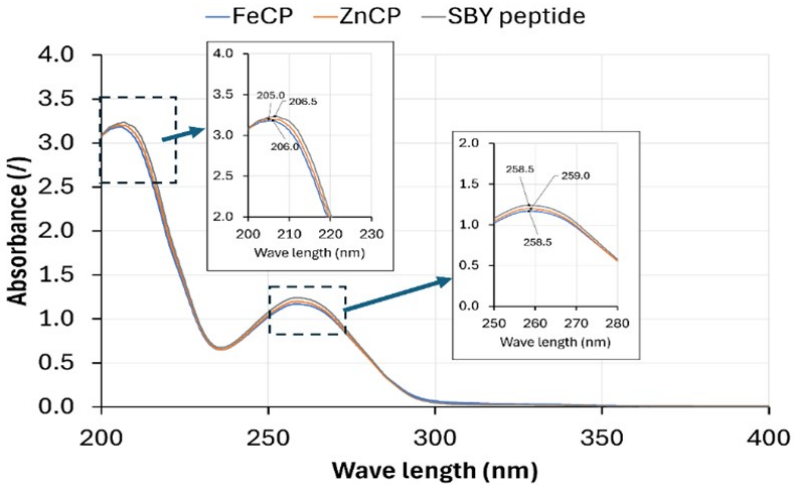

Figure 9. UV-Vis spectra of SBY peptide ≤ 3 kDa fraction and its metal chelating complexes with iron (FeCP) or zinc (ZnCP)

Changes in the FTIR absorption peaks of the carboxyl and amide groups were indicative of the interactions between metal ions and organic ligand such as peptides

(Wang et al., 2012). In this study, the FTIR spectrum of FeCP and ZnCP were compared to that of the SBY peptide (Fig. 10). The peak at 1,600.63 cm^{-1} of the SBY peptide indicated the stretching vibration of C=O of the amide-I group. It was shifted to 1,616.06 cm^{-1} and 1,594.84 cm^{-1} in the spectrum of FeCP or ZnCP, respectively. It suggested that the C=O of amide-I was a binding site for iron and zinc ions (Sun et al., 2017; Qu et al., 2022).

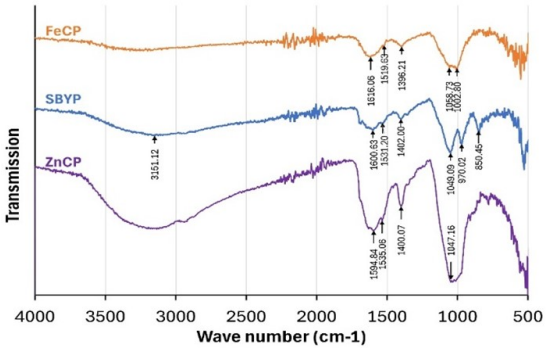

Figure 10. FTIR spectra of SBY peptide ≤ 3 kDa fraction (SBYP) and its metal chelating complexes with iron (FeCP) or zinc (ZnCP)

The peak of SBY peptide at 1,531.2 cm^{-1} corresponded to the bending of N-H or stretching of C-N from amide-II groups (Sun et al., 2023). After being chelated with iron or zinc, this peak migrated to 1,519.63 cm^{-1} and 1,535.06 cm^{-1}, respectively. Lin et al. (2021) also observed the interaction between amide-II groups and iron (II) by bending of N-H and stretching of C-N. Similar conclusions can be found by comparing the FTIR spectra of the peptide from egg yolk and its iron chelating complex (Liu et al., 2023).

Several studies have confirmed the role of carboxyl groups of amino acid residues as binding sites of metal ions (Wang et al., 2023). The peak belonging to the carboxyl group shifted from 1,402.00 cm^{-1} to 1,396.21 cm^{-1} and 1,400.07 cm^{-1} when the SBY peptide is chelated with iron and zinc, respectively. Zhao et al. (2024) suggested this variation may result from the replacement of H with zinc, while Qu et al. (2022) concluded that the iron chelating site was related to the C-terminal carboxyl of the peptide. The peak of the SBY peptide at 1,049.09 cm^{-1} shifted to 1,058.73 cm^{-1} and 1,047.16 cm^{-1} after being chelated with iron or zinc, respectively. In general, it indicated the stretching vibration of the C–N bonds of amide-I groups when interacted with metal ion as stated (Zhang et al., 2018).

Particle size distribution

The volume weighted particle size distribution of the SBY peptide and its chelated complex is illustrated in Figure 11. It was observed that the binding of Fe^{2+} to SBY peptide lead to a strong increase in particle size, from a monomodal distribution peaked at ~1 nm of SBY peptide to a multimodal distribution ranged from 20 to well under 1,000 nm. This suggests that several Fe^{2+} ions may bridge peptide chains together to form a large agglomerate, which is consistence with reported results from the literature (Fan et al., 2023; Ding et al., 2024). By contrast, the size distribution of the ZnCP sample showed almost no change compared to the SBY peptide. The nanosize of ZnCP implies a high permeability over the intestinal mucosa during digestion. This will be carefully investigated in our future research.

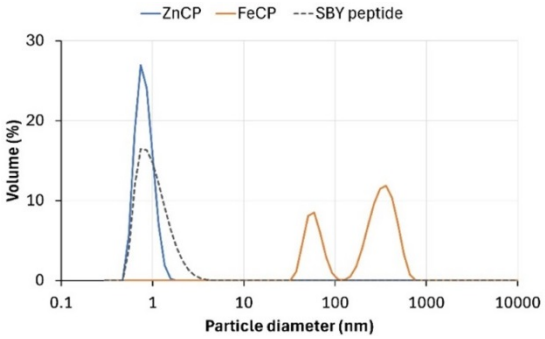

Figure 11. Particle size distribution of SBY peptide (≤ 3 kDa fraction) and its metal chelating complexes with iron (FeCP) or zinc (ZnCP)

CONCLUSION

In this study, proteins from spent brewer's yeast were successfully extracted using mechanical milling and autolysis. It was proved that both protein concentration and the

degree of hydrolysis actively alleviated the iron (II) and zinc (II) chelating ability. Moreover, the crossflow filtration method was applied, and the peptide fraction of the lowest molecular weight (≤ 3 kDa) possesses the highest iron (II) and zinc (II) chelating ability. Results also pointed out that pH 7.0 was the best condition for the chelating reaction of both FeCP and ZnCP. The reaction between iron (II) and SBY peptide required significantly higher temperature and longer reaction time than that of zinc (II). Besides, high doses of metal ions may improve the amount of chelated metal but also decrease the chelating yield. FTIR analysis suggested the interaction between iron and zinc ions and SBY peptide at positions such as C=O of the carboxyl group and at C-N or N-H of both amide-I and amide-II groups.

Acknowledgements: The authors would like to thank the Ministry of Education and Training for providing funding for project B2023-BKA-17 to pursue this research.

REFERENCES

Abbaspour N., Hurrell R., Kelishadi R., 2014. Review on iron and its importance for human health. *J Res Med Sci*, 19(2): 164−174.

Athira S., Mann B., Sharma R., Pothuraju R., Bajaj R. K., 2021. Preparation and characterization of iron-chelating peptides from whey protein: An alternative approach for chemical iron fortification. *Food Res Int*: 141. https://doi.org/ 10.1016/j.foodres.2021.110133

Caetano-Silva M. E., Bertoldo-Pacheco M. T., Paes-Leme A. F., Netto F. M., 2015. Iron-binding peptides from whey protein hydrolysates: Evaluation, isolation and sequencing by LC–MS/MS. *Food Res Int*, 71: 132−139. https://doi.org/10.1016/ j.foodres.2015.01.008

Ding X., Li H., Xu M., Li X., Li M., 2024. Peptide composition analysis, structural characterization, and prediction of iron binding modes of small molecular weight peptides from mung bean. *Food Res Int*, 175: 113735. https://doi.org/10.1016/ j.foodres.2023.113735

Fan C., Wang X., Song X., Sun R., Liu R., Sui W., Jin Y., Wu T., Zhang M., 2023. Identification of a novel walnut Iron chelating peptide with potential high antioxidant activity and analysis of its possible binding sites. *Foods*, 12(1). https://doi.org/10.3390/foods12010226

Fang S., Ruan G., Hao J., Regenstein J. M., Wang F., 2020. Characterization and antioxidant properties of Manchurian walnut meal hydrolysates after calcium chelation. *LWT*, 130: 109632. https://doi.org/10.1016/j.lwt.2020.109632

Friedman M., 2004. Applications of the ninhydrin reaction for analysis of amino acids, peptides, and proteins to agricultural and biomedical sciences. *J Agric Food Chem*, 52: 385−406. https://doi.org/ 10.1021/jf030490p

Fu T., Zhang S., Sheng Y., Feng Y., Jiang Y., Zhang Y., Yu M.,Wang C., 2020. Isolation and characterization of zinc-binding peptides from mung bean protein hydrolysates. *Eur Food Res Technol*, 246(1): 113−124. https://doi.org/10.1007/ s00217-019-03397-8

Guo H., Yu Y., Hong Z., Zhang Y., Xie Q., Chen H., 2021. Effect of collagen peptide-chelated zinc nanoparticles from Pufferfish skin on zinc bioavailability in rats. *J Med Food*, 24(9): 987−996. https://doi.org/ 10.1089/jmf.2021.K.0038

Jacob F. F., Hutzler M., Methner F.-J., 2019. Comparison of various industrially applicable disruption methods to produce yeast extract using spent yeast from top-fermenting beer production: influence on amino acid and protein content. *Eur Food Res Technol*, 245(1): 95−109. https://doi.org/10.1007/s00217-018-3143-z

Jaeger A., Arendt E. K., Zannini E., Sahin A. W., 2020. Brewer's spent yeast (BSY), an underutilized brewing by-product. *Fermentation*, 6(4). https://doi.org/ 10.3390/fermentation6040123

Jiang S., Dong W., Zhang Z., Xu J., Li H., Zhang J., Dai L., Wang S., 2022. A new iron supplement: The chelate of pig skin collagen peptide and Fe(2+) can treat iron-deficiency anemia by modulating intestinal flora. *Front Nutr*, 9: 1055725. https://doi.org/10.3389/fnut.2022.1055725

Li C., Bu G., Chen F., Li T., 2020. Preparation and structural characterization of peanut peptide–zinc chelate. *CYTA J Food*, 18(1): 409−416. https://doi.org/ 10.1080/19476337. 2020.1767695

Lin S., Hu X., Li L., Yang X., Chen S., Wu Y., Yang S., 2021. Preparation, purification and identification of iron-chelating peptides derived from tilapia (Oreochromis niloticus) skin collagen and characterization of the peptide-iron complexes. *LWT*, 149: 111796. https://doi.org/ 10.1016/j.lwt.2021.111796

Liu D., Ding L., Sun J., Boussetta N., Vorobiev E., 2016. Yeast cell disruption strategies for recovery of intracellular bio-active compounds. *Innov Food Sci Emerg Technol*, 36: 181−192. https://doi.org/ 10.1016/j.ifset.2016.06.017

Liu W. Y. Y., Ren J., Qin X. Y. Y., Zhang X. X. X., Wu H. S. S., Han L. J., 2024. Structural identification and combination mechanism of iron (II)–chelating Atlantic salmon (Salmo salar L.) skin active peptides. *J Food Sci Technol*, 61(2): 340−352. https://doi.org/10.1007/s13197-023-05845-6

Liu Y., Wang Z., Kelimu A., Korma S. A., Cacciotti I., Xiang H., Cui C., 2023. Novel iron-chelating peptide from egg yolk: Preparation, characterization, and iron transportation. *Food Chem X*: 18. https://doi.org/10.1016/j.fochx.2023.100692

Lv Y., Wei K., Meng X., Huang Y., Zhang T., Li Z., 2017. Separation and identification of iron-chelating peptides from defatted walnut flake by nanoLC-ESI–MS/MS and de novo sequencing. *Process Biochem*, 59: 223−228. https://doi.org/10.1016/j.procbio.2017.05.010

Maret W., 2004. Zinc and sulfur: a critical biological partnership. *Biochem*, 43(12): 3301−3309. https://doi.org/10.1021/bi036340p

Mirzaei M., Mirdamadi S., Aminlari M., Hoseini E., 2015. Characterization of yeast protein enzymatic hydrolysis and autolysis in *Saccharomyces cerevisiae* and *Kluyveromyces marxianus*. *Journal of food biosiences and technology*.

Oliveira A. S., Ferreira C. M. H., Pereira J. O., Sousa S., Faustino M., Durão J., Pereira A. M., Pintado M. E., Carvalho A. P., 2023. Production of iron-peptide complexes from spent yeast for nutraceutical industry. *Chem Eng Res Des*, 140: 200−211. https://doi.org/10.1016/j.fbp.2023.06.006

Peng B., Chen Z., Wang Y., 2023. Preparation and characterization of an oyster peptide–zinc complex and its antiproliferative activity on HepG2 cells. *Mar Drugs*, 21(10). https://doi.org/10.3390/md21100542

Podpora B., Świderski F., Sadowska A., Rakowska R., Wasiak-Zys G. J. C. J. o. F. S., 2016. Spent brewer's yeast extracts as a new component of functional food. *Czech J Food Sci*, 34(6): 554−563. https://doi.org/10.17221/419/2015-CJFS

Qu W., Feng Y., Xiong T., Li Y., Wahia H., Ma H., 2022. Preparation of corn ACE inhibitory peptide-ferrous chelate by dual-frequency ultrasound and its structure and stability analyses. *Ultrason Sonochem*: 83. https://doi.org/10.1016/j.ultsonch.2022.105937

Shi Q., Wei M., Chen H., Gao J., Tong P., 2021. Desalination of duck egg white by biocoagulation to obtain peptide-ferrous chelate as iron delivery system: Preparation, characterization, and Fe2+ release evaluation in vitro. *J Food Sci*, 86(10): 4678−4690. https://doi.org/ 10.1111/1750-3841.15902

Sun L. M., Yu B., Luo Y. H., Zheng P., Huang Z., Yu J., Mao X., Yan H., Luo J., He J., 2023. Effect of small peptide chelated iron on growth performance, immunity and intestinal health in weaned pigs. *Porcine*

Health Manag, 9(1). https://doi.org/10.1186/s40813-023-00327-9

Sun N., Cui P., Li D., Jin Z., Zhang S., Lin S., 2017. Formation of crystalline nanoparticles by iron binding to pentapeptide (Asp-His-Thr-Lys-Glu) from egg white hydrolysates. *Food Funct*, 8(9): 3297−3305. https://doi.org/10.1039/c7fo00843k

Sun X., Sarteshnizi R. A., Boachie R. T., Okagu O. D., Abioye R. O., Pfeilsticker Neves R., Ohanenye I. C., Udenigwe C. C., 2020. Peptide–mineral complexes: understanding their chemical interactions, bioavailability, and potential application in mitigating micronutrient deficiency. *Foods*, 9(10). https://doi.org/10.3390/foods9101402

Udechukwu M. C., Downey B., Udenigwe C. C., 2018. Influence of structural and surface properties of whey-derived peptides on zinc-chelating capacity, and in vitro gastric stability and bioaccessibility of the zinc-peptide complexes. *Food Chem*, 240: 1227−1232. https://doi.org/10.1016/j.foodchem.2017.08.063

Vieira E. F., Carvalho J., Pinto E., Cunha S., Almeida A. A., Ferreira I. M. P. L. V. O., 2016. Nutritive value, antioxidant activity and phenolic compounds profile of brewer's spent yeast extract. *J Food Compost Anal*, 52: 44−51. https://doi.org/10.1016/j.jfca. 2016.07.006

Wang B., Xiao S., Zhou G., Wang J., 2023. Novel casein-derived peptide-zinc chelate: zinc chelation and transepithelial transport characteristics. *J Agric Food Chem*, 71(18): 6978–6986. https://doi.org/10.1021/acs.jafc.3c00001

Wang C., Li B., Li H., 2014. Zn(II) chelating with peptides found in sesame protein hydrolysates: Identification of the binding sites of complexes. *Food Chem*, 165: 594−602. https://doi.org/10.1016/j.foodchem.2014.05.146

Wang L., Chen S., Liu R., Wu H., 2012. A novel hydrolytic product from flesh of Mactra veneriformis and its bioactivities in calcium supplement. *J Ocean Univ China*, 11(3): 389−396. https://doi.org/10.1007/s11802-012-1960-4

Wang T., Lin S., Cui P., Bao Z., Liu K., Jiang P., Zhu B., Sun N., 2020. Antarctic krill derived peptide as a nanocarrier of iron through the gastrointestinal tract. *Food Biosci*, 36: 100657. https://doi.org/10.1016/j.fbio.2020.100657.

Wang X., Li M., Li M., Mao X., Zhou J., Ren F., 2011. Preparation and characteristics of yak casein hydrolysate-iron complex. *Int J Food Sci Technol*, 46(8): 1705−1710. https://doi.org/10.1111/j.1365-2621.2011.02672.x

Xu B., Wang X., Zheng Y., Shi P., Zhang Y., Liu Y., Long N., 2022. Millet bran globulin hydrolysate derived tetrapeptide-ferrous chelate: Preparation, structural characterization, security prediction in silico, and stability against different food processing conditions. *LWT*: 165. https://doi.org/10.1016/j.lwt.2022.113673

Yuanqing H., Pengyao Y., Yangyang D., Min C., Rui G., Yuqing D., Haihui Z., Haile M., 2021. The preparation, antioxidant activity evaluation, and iron-deficient anemic improvement of oat (*Avena sativa* L.) peptides–ferrous chelate. *Front Nutr*: 8. https://doi.org/10.3389/fnut.2021.687133

Zhang J., Ye Z., 2022. Pentapeptide-zinc chelate from sweet almond expeller amandin hydrolysates: structural and physicochemical characteristics, stability and zinc transport ability in vitro. *Molecules*, 27(22). https://doi.org/10.3390/molecules27227936

Zhang Y., Ding X., Li M., 2021. Preparation, characterization and in vitro stability of iron-chelating peptides from mung beans. *Food Chem*: 349. https://doi.org/10.1016/j.foodchem.2021.129101

Zhang Z., Sun J., Li Y., Yang K., Wei G., Zhang S., 2023. Ameliorative effects of pine nut peptide-zinc chelate (Korean pine) on a mouse model of Alzheimer's disease. *Exp Gerontol*: 183. https://doi.org/10.1016/j.exger.2023.112308

Zhang Z., Zhou F., Liu X., Zhao M., 2018. Particulate nanocomposite from oyster (Crassostrea rivularis) hydrolysates via zinc chelation improves zinc solubility and peptide activity. *Food Chem*, 258: 269−277. https://doi.org/10.1016/j.foodchem.2018.03.030

Zhao F., Hou W., Guo L., Wang C., Liu Y., Liu X., Min W., 2024. Novel strategy to the characterization and enhance the glycemic control properties of walnut-derived peptides via zinc chelation. *Food Chem*: 441. https://doi.org/10.1016/j.foodchem.2023.138288

Zheng Y., Guo M., Cheng C., Li J., Li Y., Hou Z., Ai Y., 2023. Structural and physicochemical characteristics, stability, toxicity and antioxidant activity of peptide-zinc chelate from coconut cake globulin hydrolysates. *LWT*: 173. https://doi.org/10.1016/j.lwt.2022.114367